*Desalination and Water Treatment*
www.deswater.com

doi: 10.5004/dwt.2021.27400

229 (2021) 343–351
July

# Removal of Cr(VI) from aqueous solution by using polyaniline/polycarbonates nanofibers composite: central composite design, isotherm, and error analysis

Shurooq Sabah Kadhim, Ruba Fahmi Abbas*, Safanah Sahib Jaafar

*Department of Chemistry, College of Science, Al-Mustansiriyah University, Baghdad, Iraq, emails: rubaf1983@uomustansiriyah.edu.iq (R.F. Abbas), shrooqalshamis@gmail.com (S.S. Kadhim), dr.safana@uomustansiriyah.edu.iq (S.S. Jaafar)*

Received 10 December 2020; Accepted 5 May 2021

**ABSTRACT**

Polyaniline/polycarbonates (PANI/PC) nanofibers composite were synthesized chemically for the removal of Cr(VI) from an aqueous solution. The nanofibers were characterized using X-ray diffraction (XRD) and scanning electron microscopy (SEM). Central composite design with response surface methodology (CCD-RSM) was used for optimized some factors such as pH, the weight of PANI/PC, temperature, and contact time. The best removal (98.8%) occurred under pH 2, the weight of PANI/PC 0.05, temperature 25°C, and contact time 60 min. The high value of $R^2$ and minimized value of error functions ($\chi^2$, $\chi^2_{red}$, and $G^2$) indicated that the Freundlich isotherm model was found to be the better model rather than Langmuir and Temkin models. According to the results of XRD and SEM, affected factors using CCD-RSM, isotherm model, and error functions were involved in the adsorption process. All the results indicated that PANI/PC nanofibers composite could be used as a promising surface for the removal of Cr(VI).

*Keywords:* CCD-RSM; Removal Cr(VI); PANI/PC nanofibers; Log-likelihood ($G^2$)

## 1. Introduction

Heavy metals pollution is a worldwide issue. The industrial process such as mining of metal ores, electroplating, leather tanning, and textile dyeing give rise to increased pollution by heavy metals [1], these pollutants are present in many products such as personal care products, whitening toothpaste, pesticides, food, and many consumer products [2,3]. Cr(VI) is about 1,000 times more poisonous than other Cr forms. Cr(VI) is a stable form that leads to liver damage and skin ulceration identified by the Environmental Protection Agency of the USA [4,5].

Many classical methods have been used to remove Cr(VI) like ion exchange [6], membrane separation [7], reverse osmosis [8], microbial remediation [9], coagulation and filtration [10], chemical precipitation [11]. Most of these methods are high cost, limited, and poor stable. On the other hand, some of them give rise to increased water hardness and toxic metal ions as secondary pollutants [12]. Adsorption is a famous method used for removing pollutants from the environment; this method is easy to use, a low-cost, and non-toxic method [13].

Waste plastic bottles are one of the famous polymers used in the world, the major plastic and widely used in the manufacture is polycarbonates (PC) [14]. Polyaniline (PANI) and its composites are widely used because of their low cost, high environmental stability, and ease of preparation [15]. Many papers have been published on the synthesis of the PANI nanocomposites with different materials like poly(sulfonated styrene) [16], ZnO nanorods [17], $MnO_2$ [18], gold [19], graphene oxide/polyvinyl alcohol [20], carbon nanotube [21], and coated bacterial cellulose (BC) [22]. In this paper, synthesis and characterization of PANI and its nanocomposites with PC by X-ray diffraction (XRD) and scanning electron microscopy (SEM), then the new PANI/PC nanofibers composite is used for the removal of

* Corresponding author.

Cr(VI) from an aqueous solution. On the other hand, central composite design (CCD) and response surface methodologies (RSM) are used for the optimization of factors (pH, the weight of PANI/PC nanofibers, temperature, and contact time). Adsorption isotherms and error analysis are discussed.

## 2. Materials and methods

### 2.1. Apparatus

UV-visible spectrophotometer (Cary 100, VARIAN), SEM (Philips XL series 30), a shaking water bath (BS-11), XRD (6000, SHIMADZU), and pH meter (Hanna) were used in this study.

### 2.2. Treatment of polycarbonate waste bottle

Polycarbonate (PC) waste bottles were grounded by a laboratory-scale grinder to 200 mm particle size, the ground PC washed several times with distilled water and then with acetone to get rid of impurities, the PC particles then dried in a vacuum oven at the 50°C for overnight and keep in tightly wrapped containers.

### 2.3. Preparation of polyaniline/polycarbonate nanofibers composite

4.5 mL of aniline solution was added to 100 mL of 1 M HCl, then added 20 g of ground polycarbonate (PC) waste bottles, the mixture was mixed well by using a magnetic stirrer for 1 h.

11.5 g ammonium peroxide disulfate (APS) was used as an oxidizing agent and 100 mL of 1 M HCl as a dopant agent. After 3 h, the product was filtered and washed with D.W, ethanol, and acetone to remove unreacted aniline and impurities, then dried in an oven at 50°C for 6 h and stored in a sealed container.

### 2.4. Central composite design

Four factors (pH, the weight of PANI/PC nanofibers composite, and temperature and time) were employed for the removal of Cr(VI) by using PANI/PC nanofibers composite as a new economic absorbent. Each factor was divided into five levels ($-\alpha$, –1, 0, +1, and $+\alpha$) as shown in Table 1 [23].

Table 2 shows 30 experiments ($N = 30$), these experiments were achieved by using CCD design by using the equation ($N = 2^4 + (2 \times 4) + 6 = 30$), where $2^4$ is the factorial point, ($2 \times 4$) is the axial point and 6 is the central point [24].

### 2.5. Adsorbent development

A stock solution of 1,000 mg/L of $K_2CrO_4$ was prepared by dissolving 2.8288 g of $K_2CrO_4$ in 1,000 mL of D.W. pH values were adjusted by using 0.01 M HCl and 0.01 M NaOH. Adsorption of Cr(VI) using new surface PANI/PC nanofibers composite was carried by studying various adsorption factors namely: pH, the weight of PANI/PC nanofibers as a new absorbent, temperature, and time. For this purpose, a weighed of PANI/PC nanofibers (0.05 g) were mixed with a 25 mL of (30 mg/L) Cr(VI) solution in 25 mL volumetric flask, then added a few drops of 0.01 M HCl for obtained pH of solution 2. The mixture was agitated at a constant time of 60 min by using a shaking water bath at a constant temperature 25°C, which was more than enough to achieve equilibrium. Isotherm experiments were done by using six different of Cr(VI) initial concentrations (10, 20, 30, 40, 50, and 60 mg/L) at different temperatures (25°C, 35°C, and 45°C). The final concentration of Cr(VI) was determined by using a UV-visible spectrophotometer at 372 nm.

Table 1
Variables and levels considered for removal Cr(VI) adsorption onto PANI/PC nanofibers

| Variables (unit) | $-\alpha$ | Low | Center | High | $+\alpha$ |
|---|---|---|---|---|---|
| pH | 2 | 8 | 4 | 2 | 10 |
| Wt. of PANI/PC (mg) | 0.25 | 0.5 | 0.2 | 0.05 | 0.65 |
| Temperature (°C) | 15 | 45 | 35 | 25 | 55 |
| Time (min) | 20 | 200 | 120 | 60 | 260 |

Removal percentage ($R$ %) of Cr(VI) is defined as follows:

$$R\% = \frac{\left(C_0 - C_e\right)}{C_0} \times 100 \quad (1)$$

where $C_0$ (mg/L) is the initial concentration of Cr(VI), $C_e$ (mg/L) is the final concentration of Cr(VI).

Three isotherm models were used in this study, namely: Langmuir, Freundlich, and Temkin (Table 3).

### 2.6. Error functions

Chi-square ($\chi^2$), reduced chi-square ($\chi^2_{red}$), and log-likelihood ($G^2$) were used in this study as error functions (Table 4).

## 3. Results and discussion

### 3.1. SEM and XRD analysis

SEM and XRD were applied for characterizing and study the preparation of PANI/PC nanofibers. XRD patterns (Fig. 1A) show one peak appears at $2\theta = 21°$ for amorphous PANI [31]. On the other hand, one peak appears at $2\theta = 26°$ with PANI peak was disappeared proving the formation of PANI/PC nanofibers (Fig. 1B).

SEM image (Fig. 2) was applied for surface characteristics and morphological prepared of PANI, PC, and PANI/PC nanofibers. Fig. 2A shows pure PANI exhibits a coral-like structure; Fig. 2B shows the smooth surface of a PC and Fig. 2C and E show tubular surface PANI/PC nanofibers. This indicates that PC nanoparticles are uniformly distributed in PANI [32].

### 3.2. Model development and factors effect on Cr(VI) removal

Table 1 shows a maximum Cr(VI) removal of 98.8 was achieved under the optimum pH of 2, the weight of PANI/PC nanofibers 0.05 g, temperature 25°C, and contact

Table 2
CCD matrix used in the present study

| Run | Coded factor | | | | Actual factor | | | | Experimental recovery% | Predicted recovery% |
|---|---|---|---|---|---|---|---|---|---|---|
| | pH | Wt. | Temperature | Time | pH | Wt. | Temperature | Time | | |
| | $x_1$ | $x_2$ | $x_3$ | $x_4$ | $X_1$ | $X_2$ | $X_3$ | $X_4$ | | |
| 1 | 0 | 0 | 0 | 0 | 4 | 0.2 | 35 | 120 | 49.7 | 48.6 |
| 2 | +1 | –1 | –1 | –1 | 8 | 0.05 | 25 | 60 | 31.3 | 29.1 |
| 3 | 0 | 0 | –α | 0 | 4 | 0.2 | 15 | 120 | 44.7 | 51.6 |
| 4 | +1 | +1 | –1 | –1 | 8 | 0.5 | 25 | 60 | 23.5 | 25.5 |
| 5 | –1 | +1 | –1 | –1 | 2 | 0.5 | 25 | 60 | 80.6 | 79.2 |
| 6 | –1 | +1 | +1 | +1 | 2 | 0.5 | 45 | 200 | 72.3 | 73.3 |
| 7 | +1 | +1 | +1 | –1 | 8 | 0.5 | 45 | 60 | 24.3 | 22.7 |
| 8 | 0 | 0 | 0 | 0 | 4 | 0.2 | 35 | 120 | 50.8 | 48.6 |
| 9 | –α | 0 | 0 | 0 | 2 | 0.2 | 35 | 120 | 74.6 | 78.2 |
| 10 | 0 | 0 | 0 | 0 | 4 | 0.2 | 35 | 120 | 49.5 | 48.6 |
| 11 | 0 | 0 | 0 | 0 | 4 | 0.2 | 35 | 120 | 50.2 | 48.6 |
| 12 | –1 | +1 | –1 | +1 | 2 | 0.5 | 25 | 200 | 77.4 | 76.1 |
| 13 | +α | 0 | 0 | 0 | 10 | 0.2 | 35 | 120 | 18.3 | 18.7 |
| 14 | –1 | –1 | +1 | –1 | 2 | 0.05 | 45 | 60 | 70.7 | 79.6 |
| 15 | 0 | 0 | 0 | 0 | 4 | 0.2 | 35 | 120 | 47.6 | 48.6 |
| 16 | +1 | +1 | +1 | +1 | 8 | 0.5 | 45 | 200 | 21.3 | 23.8 |
| 17 | +1 | –1 | –1 | +1 | 8 | 0.05 | 25 | 200 | 23.8 | 37.6 |
| 18 | 0 | 0 | 0 | +α | 4 | 0.2 | 35 | 260 | 48.5 | 51.1 |
| 19 | +1 | +1 | –1 | +1 | 8 | 0.5 | 25 | 200 | 26.5 | 33.8 |
| 20 | 0 | 0 | 0 | 0 | 4 | 0.2 | 35 | 120 | 49.8 | 48.6 |
| 21 | +1 | –1 | +1 | +1 | 8 | 0.05 | 45 | 200 | 23.7 | 42.1 |
| 22 | 0 | 0 | +α | 0 | 4 | 0.2 | 55 | 120 | 41.2 | 31.4 |
| 23 | 0 | +α | 0 | 0 | 4 | 0.65 | 35 | 120 | 48.4 | 52.9 |
| 24 | –1 | +1 | +1 | –1 | 2 | 0.5 | 45 | 60 | 72.6 | 70.3 |
| 25 | 0 | 0 | 0 | –α | 4 | 0.2 | 35 | 200 | 45.4 | 51.1 |
| 26 | 0 | –α | 0 | 0 | 4 | 0.25 | 35 | 120 | 48.3 | 47.1 |
| 27 | –1 | –1 | –1 | +1 | 2 | 0.05 | 25 | 200 | 90.6 | 90.1 |
| 28 | –1 | –1 | –1 | –1 | 2 | 0.05 | 25 | 60 | 98.8 | 92.8 |
| 29 | +1 | –1 | +1 | –1 | 8 | 0.05 | 45 | 60 | 22.4 | 23.6 |
| 30 | –1 | –1 | +1 | +1 | 2 | 0.05 | 45 | 200 | 86.6 | 82.9 |

Table 3
Isotherm equations used in this study

| Isotherm | Linear equation | Plot | Parameters | Ref. |
|---|---|---|---|---|
| Langmuir | $\frac{C_e}{q_e} = \frac{1}{q_m K_L} + \frac{C_e}{q_m}$ | $(C_e/q_e)$ vs. $C_e$ | $q_m$ = 1/slope, $K_L$ = Slope/intercept | [25] |
| Freundlich | $\ln q_e = 1/n \ln C_e + \ln K_F$ | $\ln q_e$ vs. $\ln C_e$ | $K_F = e^{\text{intercept}}$, $n$ = 1/slope | [26] |
| Temkin | $q_e = q_m \ln K_T + q_m \ln C_e$ | $\ln C_e$ vs. $q_e$ | $q_m$ = slope, $K_t = e^{(\text{intercept/slope})}$ | [27] |

$K_L$ is the Langmuir constant, $K_F$ and $n$ are the Freundlich constants, $K_t$ is the Temkin constant, $1/n = 0 < (1/n) < 1$ and $q_m$ is the monolayer adsorption capacity (mg/g).

Table 4
List of error functions

| Error functions | Equations | Ref. |
|---|---|---|
| Chi-square Test ($\chi^2$) | $\sum_{i=1}^{n}\frac{\left(q_{cal}-q_{exp}\right)^2}{q_{cal}}$ | [28] |
| Reduced chi-square error ($\chi^2_{red}$) | $\frac{1}{n-p}\sum_{i=1}^{n}\frac{\left(q_{cal}-q_{exp}\right)^2}{q_{cal}}$ | [29] |
| Log-likelihood ($G^2$) | $\sum_{i=1}^{n}\left[q_{exp}\times\ln\left(\frac{q_{exp}}{q_{cal}}\right)\right]$ | [30] |

$q_{exp}$ is the experiment Cr(VI) concentration, $q_{cal}$ is the calculated Cr(VI) concentration obtained from the isotherm model, $n$(6) is the number of experimental data points in linear isotherm, and $p$(2) is the number of parameters of linear isotherm model (Langmuir, Freundlich, and Temkin).

time 60 min. The removal percent of Cr(VI) onto new surface PANI/PC nanofibers composite is expressed as the following equation by using Minitab software:

$$\text{Removal\%} = 154.9 - 24.88x_1 - 100.0x_2 - 0.239x_3 - 0.133x_4 + 1.289x_1^2 + 92.2x_2^2 - 0.00995x_3^2 + 0.000204x_4^2 + 3.77x_1x_2 + 0.0518x_1x_3 - 0.00219x_1x_4 + 0.464x_2x_3 - 0.0050x_2x_4 + 0.00240x_3x_4 \quad (2)$$

The double factors (except $x_3^2$ (temp²), $x_1x_4$ (pH × wt), and $x_2x_4$ (wt. × time)) increased Cr(VI) removal onto PANI/PC nanofibers (positive coefficient values), while the rest factors having negative coefficient values which decreased Cr(VI) removal [33].

ANOVA table of Cr(VI) removal onto PANI/PC nanofibers are listed in Table 5. A $p$-value less than 0.05 indicates that the CCD model is significant [34]. In this case, very small values of the model, $x_1$(pH), $x_1x_1$(pH)², $x_2$(wt.)², and $x_1x_2$(pH × wt) as seen in Table 5 indicated that these factors are significant, while the other factors in Table 5 are not significant (high $p$-value, $p > 0.05$).

The $p$-value of "lack of fit" is 0.01 indicated that the "lack of fit" is significant. So, it can be observed that the pH and weight of PANI/PC nanofibers play an important role in Cr(VI) removal.

The aim of the model summary table is to check the accuracy of the CCD model (Table 6). The high value of the statistical metrics ($R^2$, $R^2_{adj}$, and $R^2_{pred}$) indicating a highly significant of the CCD model. On the other hand, the low value of CV shows the accuracy and precision of the experiments [35].

A good linear regression fit between predicated removal and experimental removal, as shown in Fig. 3, indicated a good fit of the CCD model [36].

Fig. 4 shows 3D-RSM plots of removal Cr(VI) onto PANI/PC nanofibers. Fig. 4A–C show the highest Cr(VI) removal (over 80%) has been achieved based on the response surface of the $x_1x_2$, $x_1x_3$, and $x_1x_4$, while Fig. 4D–F show lowest Cr(VI) removal (less 35%), this indicated that pH factor is the most factor effected on the removal Cr(VI) onto PANI/PC nanofibers.

It seems that the mechanism of Cr(VI) ion adsorption onto PANI/PC nanofibers occurred at highly acidic media (pH 2). At this pH, the dichromate ($Cr_2O_4^{2-}$) is converted to chromate ($HCrO_4^-$), and then PANI/PC nanofibers can remove ($HCrO_4^-$) as follows [37]:

$$Cr_2O_4^{2-} + 2H^+ \rightarrow 2HCrO_4^- \quad (3)$$

$$\text{PANI/HCl(polymer)} + HCrO_4^- \rightarrow \text{PANI/}HCrO_4^-\text{(polymer)} + Cl^- \quad (4)$$

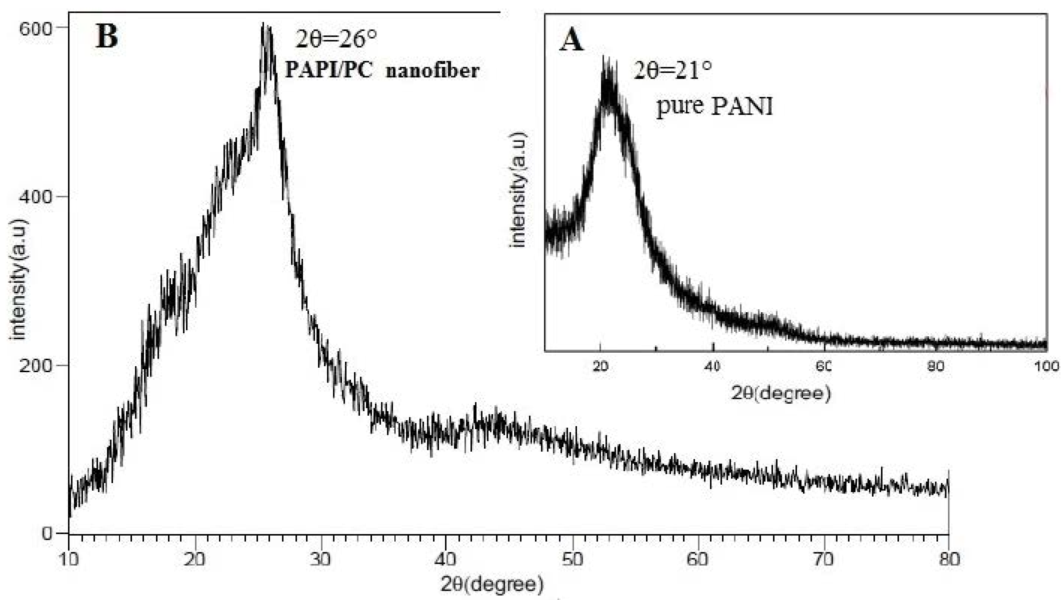


Fig. 1. XRD pattern of PANI/PC nanofibers and the inset shows XRD taken for pure PANI.

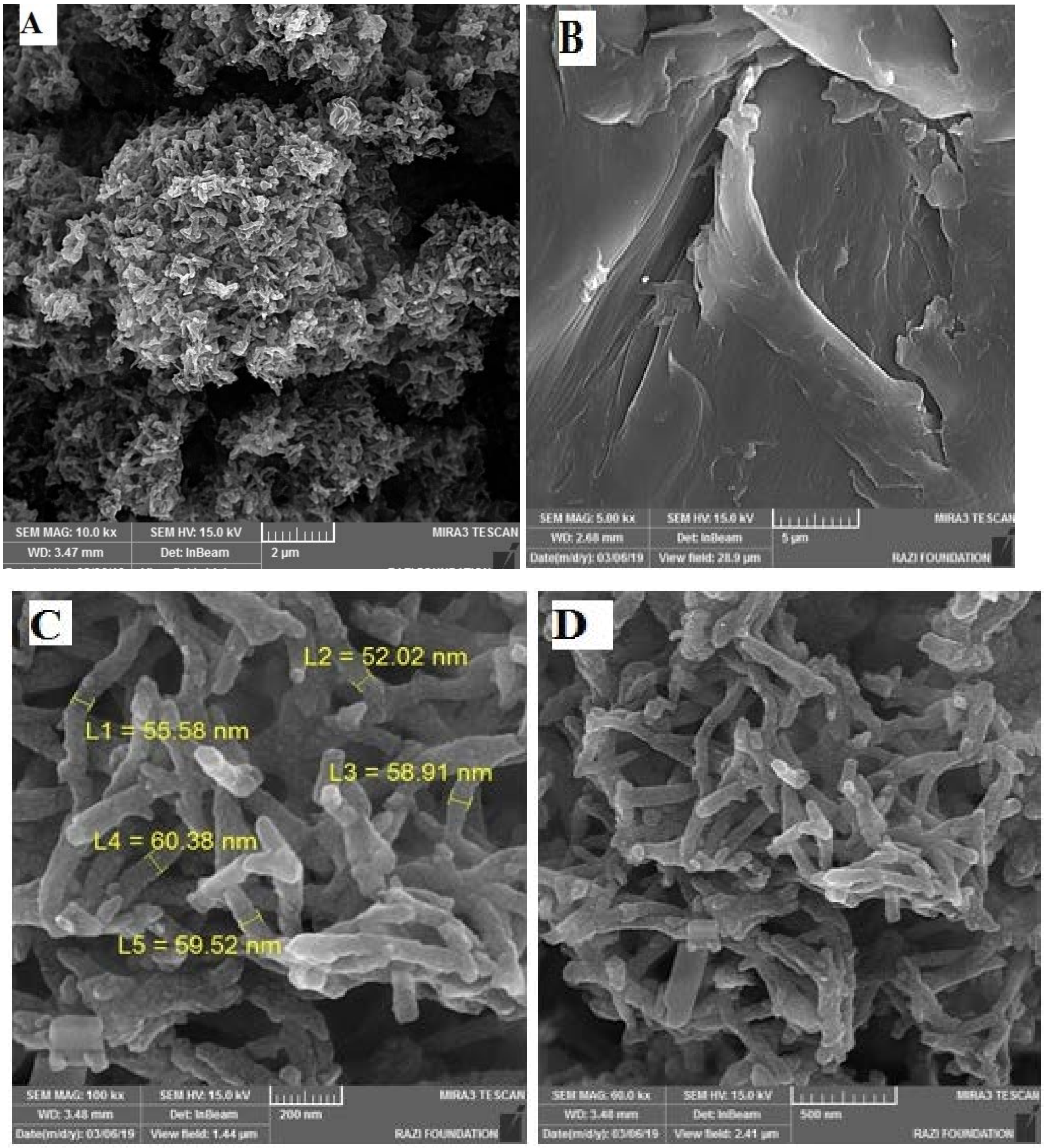


Fig. 2. SEM images of (A) PANI, (B) PC, and (C and D) PANI/PC nanofibers.

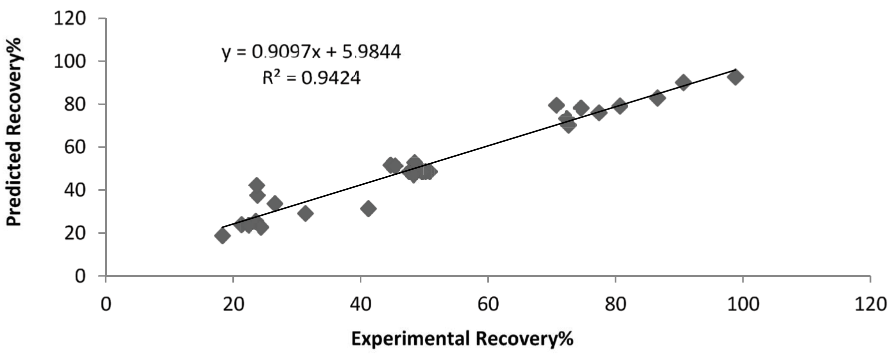


Fig. 3. Comparisons of the experimental removal% plotted vs. the predicted removal%.

Table 5
ANOVA for the removal of Cr(VI) adsorption onto PANI/PC nanofibers by CCD model

| Source | DF | Adj. SS | Adj. MS | $F$-value | $P$-value |
|---|---|---|---|---|---|
| Model | 14 | 15,128.9 | 1,080.64 | 48.29 | 0.000 |
| Linear | 4 | 4,203.0 | 1,050.75 | 46.95 | 0.000 |
| $x_1$ | 1 | 4,151.2 | 4,151.17 | 185.50 | 0.000 |
| $x_2$ | 1 | 3.7 | 3.73 | 0.17 | 0.689 |
| $x_3$ | 1 | 7.8 | 7.77 | 0.35 | 0.565 |
| $x_4$ | 1 | 0.1 | 0.06 | 0.00 | 0.958 |
| Square | 4 | 1,669.0 | 417.25 | 18.65 | 0.000 |
| $x_1x_1$ | 1 | 1,025.1 | 1,025.05 | 45.81 | 0.000 |
| $x_2x_2$ | 1 | 160.9 | 160.92 | 7.19 | 0.017 |
| $x_3x_3$ | 1 | 28.1 | 28.08 | 1.25 | 0.280 |
| $x_4x_4$ | 1 | 11.0 | 10.95 | 0.49 | 0.495 |
| 2-Way interaction | 6 | 216.9 | 36.16 | 1.62 | 0.211 |
| $x_1x_2$ | 1 | 106.2 | 106.17 | 4.74 | 0.046 |
| $x_1x_3$ | 1 | 40.1 | 40.05 | 1.79 | 0.201 |
| $x_1x_4$ | 1 | 3.4 | 3.41 | 0.15 | 0.702 |
| $x_2x_3$ | 1 | 18.1 | 18.09 | 0.81 | 0.383 |
| $x_2x_4$ | 1 | 0.1 | 0.10 | 0.00 | 0.947 |
| $x_3x_4$ | 1 | 45.4 | 45.42 | 2.03 | 0.175 |
| Error | 15 | 335.7 | 22.38 | – | – |
| Lack-of-fit | 10 | 329.8 | 32.98 | 28.14 | 0.001 |
| Pure error | 5 | 5.9 | 1.17 | – | – |
| Total | 29 | 15,464.6 | – | – | – |

$Cl^-$ ion in PANI can be exchangeable in the acid medium only (pH = 2). Thus, at lower pH, the positive charged NH group could easily absorb chromate ($HCrO_4^-$) anion. Notably, the reduction reactions consume $H^+$, which will lead to the increase of solution pH as shown in Fig. 5 [38].

### 3.3. Isotherm study and error functions

The use of adsorption isotherm models to describe the nature of the interaction between PANI/PC nanofibers and Cr(VI). Linear Langmuir isotherm (Fig. 6A) is the monolayer adsorption Cr(VI) onto PANI/PC nanofibers [39], while linear Freundlich isotherm (Fig. 6B) is the multilayer formation of Cr(VI) onto heterogeneous PANI/PC nanofibers [26], finally, linear Temkin isotherm (Fig. 6C) is used to study the adsorption heat and interaction of Cr(VI) onto PANI/PC nanofibers [27]. Error functions are used to find the best fitting of isotherm models. The purpose of used the error functions in this study to find the goodness of fit of linear isotherm models [24]. $\chi^2$ and $\chi^2_{red}$ analysis are better methods used for a measure of the best fitting of linear isotherm models [28,29], also log-likelihood (or called G-square test ($G^2$)) is a new error analysis used to calculate goodness-fit of linear isotherm models [30]. It seems from Table 7, Freundlich model appeared to be the best one when the error functions have the minimum values.

On the other hand, the Freundlich model has the highest values of ($R^2$ = 0.925) compared to other models. So the low values of error functions and the highest value of $R^2$ for the linear Freundlich model proved that this model is the preferred linear isotherm and this study is the heterogeneous nature of adsorption.

Table 6
Model summary

| CV | $R^2$ | $R^2_{adj}$ | $R^2_{pred}$ |
|---|---|---|---|
| 4.73059 | 97.83% | 95.80% | 83.70% |

CV is the coefficient of variance, $R^2$ is the coefficient of determined, $R^2_{adj}$ is the adjusted coefficient of determined, and $R^2_{pred}$ is the predicated coefficient of determined.

Table 7
Linear isotherm parameters for Cr(VI) adsorption onto PANI/PC nanofibers

| Isotherm models | Parameter | value | $\chi^2$ | $\chi^2_{red}$ | $G^2$ |
|---|---|---|---|---|---|
| Langmuir | $K_L$ | 16.75 | 14.712 | 3.678 | 1.366 |
| | $q_m$ | 14.925 | | | |
| | $R^2$ | 0.805 | | | |
| Freundlich | $K_F$ | 14.182 | 9.088 | 0.192 | 0.409 |
| | $n$ | 0.5299 | | | |
| | $R^2$ | 0.925 | | | |
| Temkin | $K_T$ | 1.990 | 12.381 | 0.327 | 0.562 |
| | $q_m$ | 24.56 | | | |
| | $R^2$ | 0.842 | | | |

### 3.4. Comparison with other studies

Table 8 shows the pH effect of PANI/PC nanofibers toward Cr(VI) removal was similar to various kinds of

Table 8
Comparison of isotherm, pH, and contact time of Cr(VI) using a new PANI/PC nanofibers with other nanofibers in the literature

| Adsorbents | Isotherm | pH | Contact time | Ref. |
|---|---|---|---|---|
| Polyacrylonitrile/polypyrrole core/shell nanofibers | Langmuir | 2 | 90 | 39 |
| PAN/ZnO-$TiO_2$ nanofibers-Mat | Langmuir | 2 | 240 | 40 |
| polypyrrole/$Fe_3O_4$ magnetic | Langmuir | 2 | 30–180 | 41 |
| Sodium alginate-polyaniline(SAP) nanofiberss | Freundlich | 2 | 60 | 42 |
| PANI/PC nanofibers | Freundlich | 2 | 60 | This study |

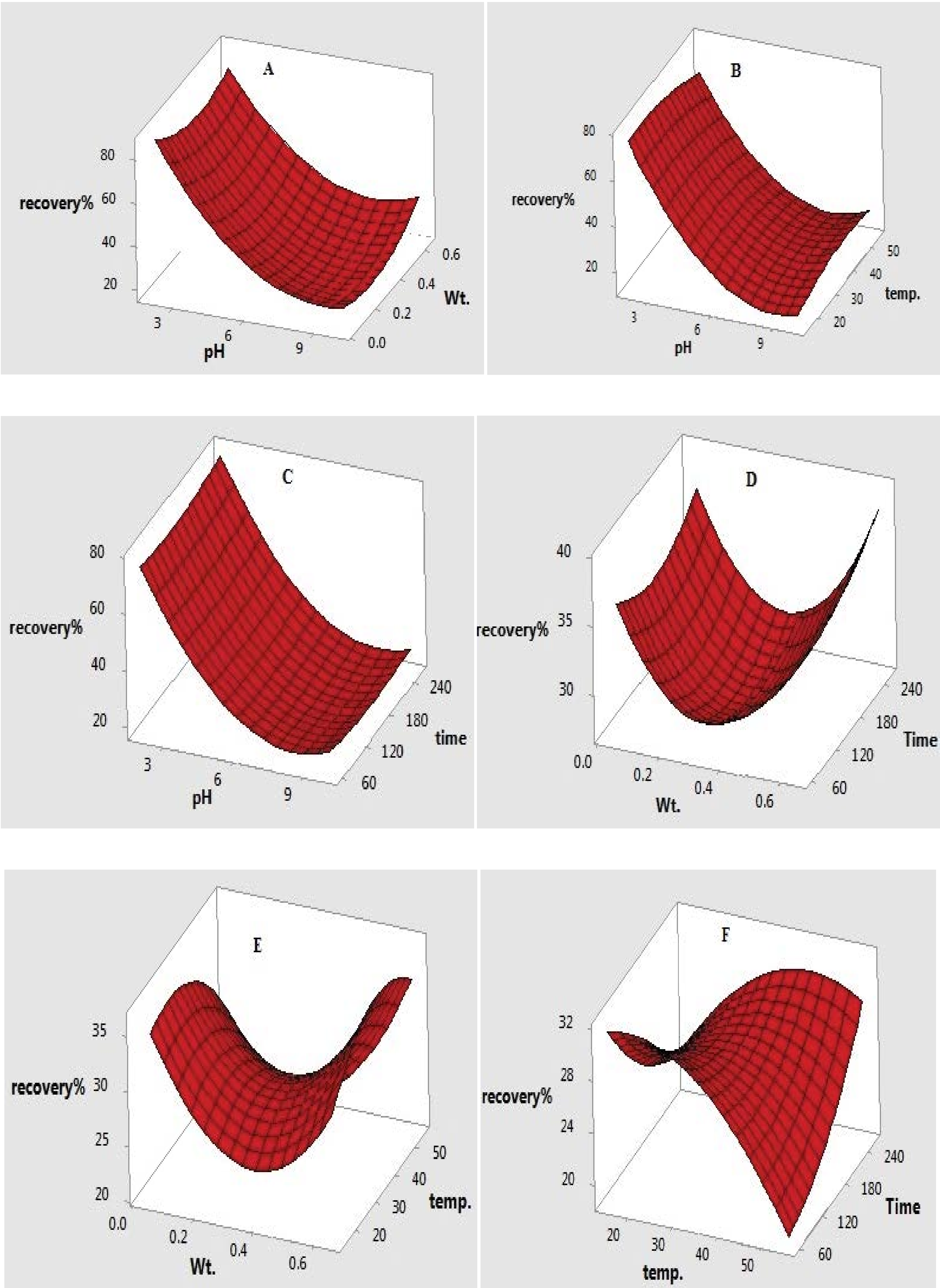


Fig. 4. 3D surface plots of Cr(VI) removal% onto PANI/PC nanofibers composite: (A) effect pH/weight (temperature 25°C and time 60 min), (B) effect pH/temperature (weight 0.05 g and time 60 min), (C) effect pH/ time (weight 0.05 g and temperature 25°C), (D) effect weight/time (pH 2 and temperature 25°C), (E) effect weight/temperature (pH 2 and time 60 min), and (F) effect temperature/ time (pH 2 and weight 0.05 g).

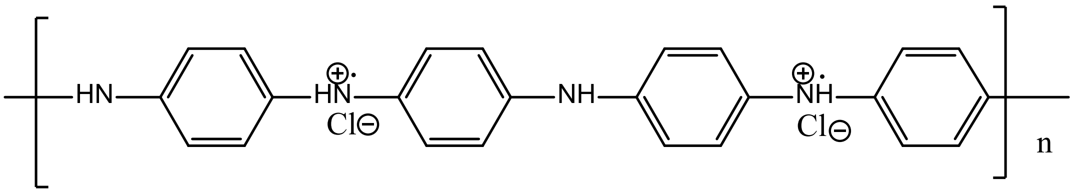


Fig. 5. Chemical structure of synthesized polyaniline (PANI).

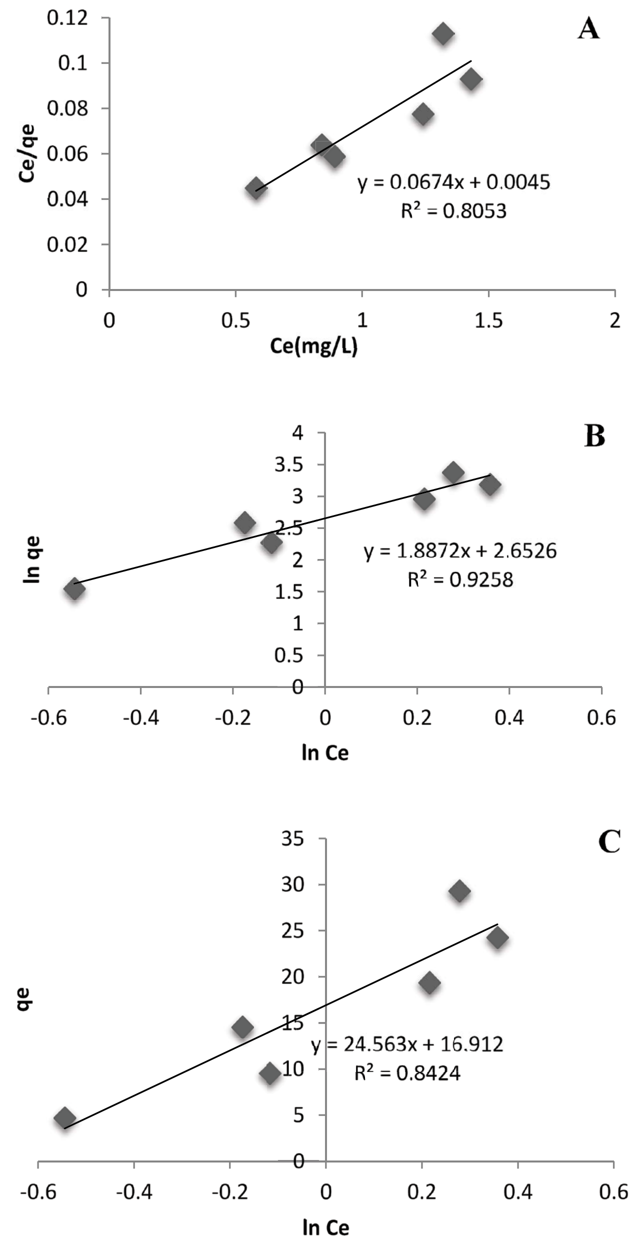


Fig. 6. (A) Langmuir, (B) Freundlich, and (C) Temkin linear isotherm for adsorption of Cr(VI) on PANI/PC nanofibers at 25°C.

adsorbents in the literature, a contact time effect was lower than in the literature and the isotherm model was found to be similar to sodium alginate-polyaniline (SAP) nanofibers adsorbent.

## 4. Conclusion

In this study, PANI/PC nanofibers were successfully used for the removal of Cr(VI) from an aqueous solution. A maximum Cr(VI) removal of 98.8 was achieved under the optimum pH of 2, the weight of PANI/PC nanofibers 0.05 g, temperature 25°C, and contact time 60 min by using CCD-RSM design. The high value of $R^2$ (0.925) and the minimized value of error functions ($\chi^2$ = 9.088), ($\chi^2_{red}$ = 0.192), and ($G^2$ = 0.409) indicated that the Freundlich isotherm model was found to be the best model rather than other models. In addition, compared with various kinds of adsorbents, the PANI/PC nanofibers had much lower time Cr(VI) removal, which indicated the possible used of PANI/PC nanofibers as an efficient adsorbent to remove Cr(VI) ion from aqueous solutions.

## Acknowledgments

We thank the University of Mustansiriyah, College of Science, Department of Chemistry for helpful in doing this work.

## References

[1] R. Fu, Y. Yang, Z. Xu, X. Zhang, X. Guo, D. Bi, The removal of chromium(VI) and lead(II) from groundwater using sepiolite-supported nanoscale zero-valent iron (S-NZVI), Chemosphere, 138 (2015) 726–734.
[2] V.V. Priyan, T. Shahnaz, E. Suganya, S. Sivaprakasam, S. Narayanasamy, Ecotoxicological assessment of micro-pollutant diclofenac biosorption on magnetic sawdust: phyto, microbial and fish toxicity studies, J. Hazard. Mater., 403 (2021) 1–13.
[3] T. Shahnaz, V. Sharma, S. Subbiah, S. Narayanasamy, Multivariate optimisation of Cr(VI), Co(III) and Cu(II) adsorption onto nanobentonite incorporated nanocellulose/chitosan aerogel using response surface methodology, J. Water Process Eng., 36 (2020) 1–12.
[4] T. Shahnaz, V.C. Padmanaban, S. Narayanasamy, Surface modification of nanocellulose using polypyrrole for the adsorptive removal of Congo red dye and chromium in binary mixture, Int. J. Biol. Macromol., 151 (2020) 322–332.
[5] H. Liu, F. Zhang, Z. Peng, Adsorption mechanism of Cr(VI) onto GO/PAMAMs composites, Sci. Rep., 9 (2019) 1–12.
[6] D. Huang, G. Wang, Z. Shi, Z. Li, F. Kang, F. Liu, Removal of hexavalent chromium in natural groundwater using activated carbon and cast iron combined system, J. Cleaner Prod., 165 (2017) 667–676.
[7] S.S. Hosseini, A. Nazif, M.A.A. Shahmirzadi, I. Ortiz, Fabrication, tuning and optimization of poly(acrilonitryle) nanofiltration membranes for effective nickel and chromium removal from electroplating wastewater, Sep. Purif. Technol., 187 (2017) 46–59.
[8] L. Lin, X. Xu, C. Papelis, T.Y. Cath, P. Xu, Sorption of metals and metalloids from reverse osmosis concentrate on drinking water treatment solids, Sep. Purif. Technol., 134 (2014) 37–45.

[9] R. Jobby, P. Jha, A.K. Yadav, N. Desai, Biosorption and biotransformation of hexavalent chromium [Cr(VI)]: a comprehensive review, Chemosphere, 207 (2018) 255–266.
[10] G. Qin, M.J. McGuire, N.K. Blute, C. Seidel, L. Fong, Hexavalent chromium removal by reduction with ferrous sulfate, coagulation, and filtration: a pilot-scale study, Environ. Sci. Technol., 39 (2005) 6321–6327.
[11] S. Stylianou, K. Simeonidis, M. Mitrakas, A. Zouboulis, M. Ernst, I.A. Katsoyiannis, Reductive precipitation and removal of Cr(VI) from groundwaters by pipe flocculation–microfiltration, Environ. Sci. Pollut. Res., 25 (2018) 12256–12262.
[12] V.E. Pakade, N.T. Tavengwa, L.M. Madikizela, Recent advances in hexavalent chromium removal from aqueous solutions by adsorptive methods, RSC Adv., 9 (2019) 26142–26164.
[13] R. Bagheri, M. Ghaedi, A. Asfaram, E.A. Dil, H. Javadian, RSM-CCD design of malachite green adsorption onto activated carbon with multimodal pore size distribution prepared from *Amygdalus scoparia*: kinetic and isotherm studies, Polyhedron, 171 (2019) 464–472.
[14] M.M. López, G.M. Barrera, J.J. del Coz-Díaz, J.E. Martínez, O. Gencel, M.C. Ribeiro, V.V. Guerrero, Polymer waste materials as fillers in polymer mortars: experimental and finite elements simulation, Case Stud. Constr. Mater., 9 (2018) 1–10.
[15] M.R. Samani, D. Toghraie, Using of polyaniline–polyvinyl acetate composite to remove mercury from aqueous media, Int. J. Environ. Res., 14 (2020) 303–310.
[16] A.R. Hopkins, D.D. Sawall, R.M. Villahermosa, R.A. Lipeles, Interfacial synthesis of electrically conducting polyaniline nanofiber composites, Thin Solid Films, 469 (2004) 304–308.
[17] A. Mostafaei, A. Zolriasatein, Synthesis and characterization of conducting polyaniline nanocomposites containing ZnO nanorods, Prog. Nat. Sci.: Mater. Int., *22* (2012) 273–280.
[18] S.A. Iranagh, L. Eskandarian, R. Mohammadi, Synthesis of $MnO_2$-polyaniline nanofiber composites to produce high conductive polymer, Synth. Metals, 172 (2013) 49–53.
[19] S. Liu, H. Xu, J. Ou, Z. Li, S. Yang, J. Wang, A feasible approach to the fabrication of gold/polyaniline nanofiber composites and its application as electrocatalyst for oxygen reduction, Mater. Chem. Phys., 132 (2012) 500–504.
[20] S. Morimune, T. Nishino, T. Goto, Poly(vinyl alcohol)/graphene oxide nanocomposites prepared by a simple eco-process, Polym. J., 44 (2012) 1056–1063.
[21] Y. Liao, C. Zhang, Y. Zhang, V. Strong, J. Tang, X.G. Li, R.B. Kaner, Carbon nanotube/polyaniline composite nanofibers: facile synthesis and chemosensors, Nano Lett., 11 (2011) 954–959.
[22] D. Müller, J.S. Mandelli, J.A. Marins, B.G. Soares, L.M. Porto, C.R. Rambo, G.M.O. Barra, Electrically conducting nanocomposites: preparation and properties of polyaniline (PAni)-coated bacterial cellulose nanofibers (BC), Cellulose, 19 (2012) 1645–1654.
[23] H. Haffad, M. Zbair, Z. Anfar, H.A. Ahsaine, H. Bouhlal, H. Khallok, Removal of reactive red-198 dye using chitosan as an adsorbent: optimization by central composite design coupled with response surface methodology, Toxin Rev., (2019) 1–13.
[24] R.F. Abbas, H.K. Hami, N.I. Mahdi, A.A. Waheb, Removal of Eriochrome black T dye by using $Al_2O_3$ nanoparticles: central composite design, isotherm and error analysis, Iran. J. Sci. Technol. Trans. A, Sci., 44 (2020) 993–1000.
[25] H.S. Mohamed, N.K. Soliman, D.A. Abdelrheem, A.A. Ramadan, A.H. Elghandour, S.A. Ahmed, Adsorption of $Cd^{2+}$ and $Cr^{3+}$ ions from aqueous solutions by using residue of *Padina gymnospora* waste as promising low-cost adsorbent, Heliyon, 5 (2019) 1–32.
[26] A.D. Delil, O. Gülçiçek, N. Gören, Optimization of adsorption for the removal of cadmium from aqueous solution using Turkish coffee grounds, Int. J. Environ. Res., 13 (2019) 861–878.
[27] Y.S. Kim, J.H. Kim, Isotherm, kinetic and thermodynamic studies on the adsorption of paclitaxel onto Sylopute, J. Chem. Thermodyn., 130 (2019) 104–113.
[28] R.F. Abbas, H.K. Hami, N.I. Mahdi, Removal of doxycycline hyclate by adsorption onto cobalt oxide at three different temperatures: isotherm, thermodynamic and error analysis, Int. J. Environ. Sci. Technol., 16 (2019) 5439–5446.
[29] S. Hokkanen, A. Bhatnagar, A. Koistinen, T. Kangas, U. Lassi, M. Sillanpää, Comparison of adsorption equilibrium models and error functions for the study of sulfate removal by calcium hydroxyapatite microfibrillated cellulose composite, Environ. Technol., 39 (2018) 952–966.
[30] M. Hadi, G. McKay, M.R. Samarghandi, A. Maleki, M. Solaimany, Prediction of optimum adsorption isotherm: comparison of chi-square and log-likelihood statistics, Desal. Water Treat., 49 (2012) 81–94.
[31] H. Xu, J. Zhang, Y. Chen, H. Lu, J. Zhuang, Electrochemical polymerization of polyaniline doped with $Cu^{2+}$ as the electrode material for electrochemical supercapacitors, RSC Adv., 4 (2014) 5547–5552.
[32] J. Ren, X. Huang, N. Wang, K. Lu, X. Zhang, W. Li, D. Liu, Preparation of polyaniline-coated polyacrylonitrile fiber mats and their application to Cr(VI) removal, Synth. Met., 222 (2016) 255–266.
[33] B. Sadhukhan, N.K. Mondal, S. Chattoraj, Optimisation using central composite design (CCD) and the desirability function for sorption of methylene blue from aqueous solution onto Lemna major, Karbala Int. J. Mod. Sci., 2 (2016) 145–155.
[34] A. Hassani, M. Kiranşan, R.D.C. Soltani, A. Khataee, S. Karaca, Optimization of the adsorption of a textile dye onto nanoclay using a central composite design, Turk. J. Chem., 39 (2015) 734–749.
[35] V. Javanbakht, S.M. Ghoreish, Application of response surface methodology for optimization of lead removal from an aqueous solution by a novel superparamagnetic nanocomposite, Adsorpt. Sci. Technol., 35 (2017) 241–260.
[36] N. Sivarajasekar, N. Mohanraj, S. Sivamani, J.P. Maran, I.G. Moorthy, K. Balasubramani, Statistical optimization studies on adsorption of ibuprofen onto Albizialebbeck seed pods activated carbon prepared using microwave irradiation, Mater. Today: Proc., 5 (2018) 7264–7274.
[37] T.S. Najim, A.J. Salim, Polyaniline nanofibers and nano-composites: preparation, characterization, and application for Cr(VI) and phosphate ions removal from aqueous solution, Arabian J. Chem., 10 (2017) S3459–S3467.
[38] R. Ansari, Application of polyaniline and its composites for adsorption/recovery of chromium(VI) from aqueous solutions, Acta Chim. Slov., 53(2006) 88–94.
[39] J. Wang, K. Pan, Q. He, B. Cao, Polyacrylonitrile/polypyrrole core/shell nanofiber mat for the removal of hexavalent chromium from aqueous solution, J. Hazard. Mater., 244 (2013) 121–129.
[40] Ş. Parlayıcı, A. Yar, E. Pehlivan, A. Avcı, ZnO-$TiO_2$ doped polyacrylonitrile nano fiber-Mat for elimination of Cr(VI) from polluted water, J. Anal. Sci. Technol., 10 (2019) 1–12.
[41] M. Bhaumik, A. Maity, V.V. Srinivasu, M.S. Onyango, Enhanced removal of Cr(VI) from aqueous solution using polypyrrole/$Fe_3O_4$ magnetic nanocomposite, J. Hazard. Mater., 190 (2011) 381–390.
[42] R. Karthik, S. Meenakshi, Removal of Cr(VI) ions by adsorption onto sodium alginate-polyaniline nanofibers, Int. J. Biol. Macromol., 72 (2015) 711–717.